

Supplementary information

Reversible Structural Transformation of Metastable Lead-Free Organic-Inorganic Hybrid Bismuth Halide Single Crystals

Yurou Zhang,^a Mehri Ghasemi,^b Xiaoming Wen,^b Minwoo Lee,^c Xiaoxia Liu,^d Yalong Jiao,^d Paul V. Bernhardt,^e EQ Han,^a Tongen Lin,^a Bo Wei Zhang,^a Kaijie Xu,^a Su-Min Lee,^f Jae Sung Yun,^{c, g} Jung-Ho Yun,^{*f} and Lianzhou Wang.^{*a}

- a. Nanomaterials Centre, School of Chemical Engineering, Australian Institute for Bioengineering and Nanotechnology (AIBN), The University of Queensland, Brisbane, 4027 Australia. E-mail: l.wang@uq.edu.au
- b. School of Science, RMIT University, Melbourne, 3000 Australia
- c. Australian Centre for Advanced Photovoltaics (ACAP), School of Photovoltaic and Renewable Energy Engineering, School of Materials Science and Engineering, University of New South Wales, Sydney, 2052 Australia
- d. College of Physics, Hebei Key Laboratory of Photophysics Research and Application, Hebei Normal University, Shijiazhuang, 050024 China
- e. School of Chemistry and Molecular Biosciences, The University of Queensland, Brisbane, 4027, Australia
- f. Air & Environment Energy Nexus (A2EN) Laboratory, Department of Environmental Science and Engineering, College of Engineering, Kyung Hee University, Yongin-si, 17104 Republic of Korea, E-mail: jungho.yun@khu.ac.kr
- g. School of Computer Science and Electronic Engineering, Advanced Technology Institute (ATI), University of Surrey, Guildford, Surrey, GU2 7XH UK

Experimental Procedures

Crystallization of PDABiI₅ single crystals

1.5 mmol of bismuth (III) oxide (Bi₂O₃, 99.9% trace metals basis, Sigma-Aldrich) and 3 mmol of Propane-1,3-diammonium iodide (PDAI₂, 99.99%, Greatcell Solar) were dissolved in 8 mL of HI aqueous solution (57 wt. % in H₂O, contains <1.5% hypophosphorous acid as a stabilizer, Sigma-Aldrich) at 115 °C with constant stirring for 2 hours. The precursor solution was then slowly cooled to 40°C in a stable and uninterrupted condition. After the crystallization was completed, crystals were filtered and dried in a vacuum oven at 80°C overnight. It should be noted that the precise control of both concentration and temperature is critical to prevent the formation of the by-product. Keeping the low-concentrated precursor at below 40°C results in the precipitation of a distinct type of single crystal, PDA₅Bi₂I₁₆, of which the crystal structure is shown in **Fig. S14** and detailed crystallographic data can be found in **Table S1**.

Large high-quality PDABiI₅ single crystals were synthesized by hydrothermal method. 4 mmol of Bi₂O₃ and 8 mmol of PDAI₂ were mixed with 25 mL of HI aqueous solution in a Teflon-lined autoclave (70 mL). The autoclave was then heated at 140 °C for 2 hours in an oven. The precursor solution was then slowly cooled to room temperature in the oven at a rate of 1°C/h. After the crystallization was completed, crystals were filtered and dried in a vacuum oven at 80°C overnight.

Structure characterizations

Powder X-ray diffraction (XRD) was performed with Bruker D8 Advance X-ray diffractometer with a Cu K α source ($\lambda=1.54\text{ \AA}$) at 45 kV and 40 mA. Single crystal XRD data were obtained on an Oxford Diffraction Gemini Ultra CCD diffractometer with a Cu source (1.5418 \AA) with the crystal cooled to 190 K with an Oxford Cryosystems Desktop Cooler. Raman spectra was tested at a laser wavelength of 785 nm using Renishaw Micro-Raman Spectroscopy System. Fourier transform infrared spectra (FTIR) were performed with Nicolet 5700.

Steady-state and time-resolved PL measurement

The time-dependent steady-state PL spectra were acquired and detected by a QE Pro fluorimeter (Ocean Optics) equipped with a thermoelectrically cooled Si CDD detector. The

TRPL was obtained by a time-correlated single-photon counting (TCSPC) technique (PicoHarp 300). For the excitation sources, a 405 nm laser is a picosecond diode laser (PicoHarp LDH laser) suitably attenuated by a neutral density filter). The excitation laser density was set at 500 mW/cm². All the measurements were conducted at room temperature. For temperature-dependent PL and TRPL, the sample was installed in a cryostat (Oxford Optistat CF-V) with a controllable temperature between 80 and 300 K using liquid nitrogen cooling.

DFT Calculations

First-principles calculations were performed based on the density functional theory (DFT) as implemented in the Vienna ab initio simulation package (VASP) code.^{1, 2} The projected augmented-wave (PAW) method was used to describe the ion-electron interaction³. The Perdew-Burke-Ernzerhof (PBE) parameterized general gradient approximation (GGA) is adopted for the electronic exchange-correlation functional.⁴ Electronic wave functions were expanded using a plane-wave basis set with an energy cutoff of 400 eV. The structures were relaxed with the conjugate-gradient method until the Hellmann-Feynman force on each atom was less than 0.05 eV/Å and the convergence criterion for the self-consistent electronic minimization loop was set to 10⁻⁴ eV. To reduce the computational load, simplified models with smaller cells were employed. The simplified crystal structure models are presented in **Fig. S6**.

AFM and KPFM measurement

KPFM measurements were performed by using NX-10 Park Systems in an ambient atmosphere. The data were acquired by using a radius of curvature of 35 nm (HA_NC/Au) cantilever and $k = 3.5 \pm 20\%$ n/m. The scan rate was 0.25 Hz and performed at 1.5 μm at 256 pixels. Sideband KPFM was utilized with the sideband's frequency of 3 kHz instead of using a frequency of 17 kHz. The KPFM data was analyzed by Gwyddion.

Supplementary figures

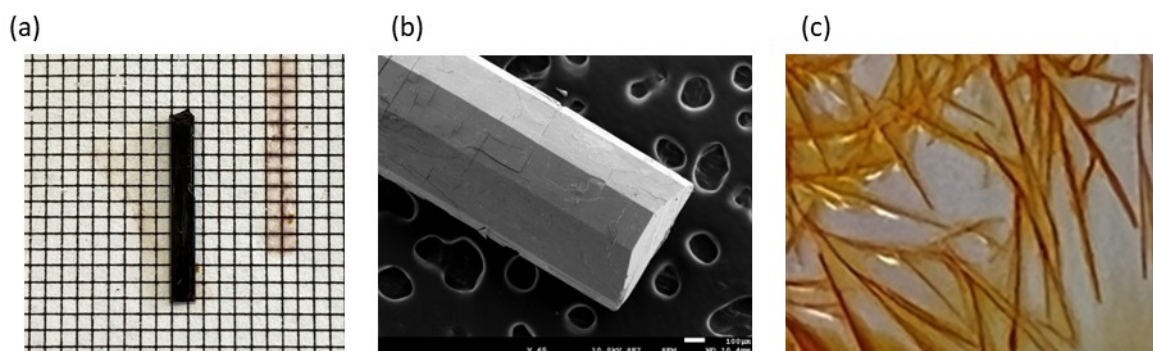


Fig. S1. (a) Photo of an as-synthesized 1D PDABi₅ single crystal. The grid size is 1 mm × 1 mm. (b) SEM image of a 1D PDABi₅ single crystal. (c) Photo of 0D PDA₂Bi₂I₁₀·2H₂O single crystals.

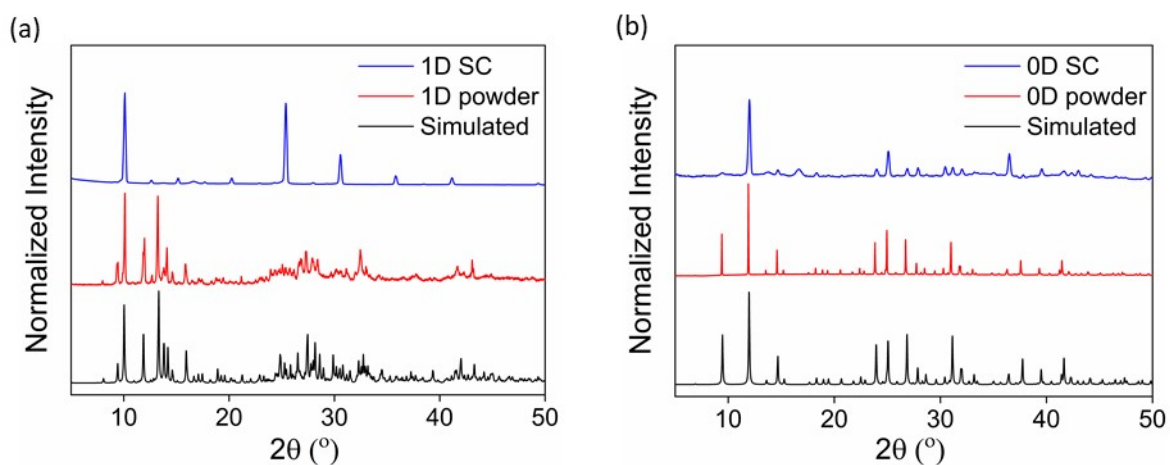


Fig. S2. XRD patterns of single crystals, powders and simulated reference patterns of (a) 1D PDABi₅ material and (b) 0D PDA₂Bi₂I₁₀·2H₂O material.

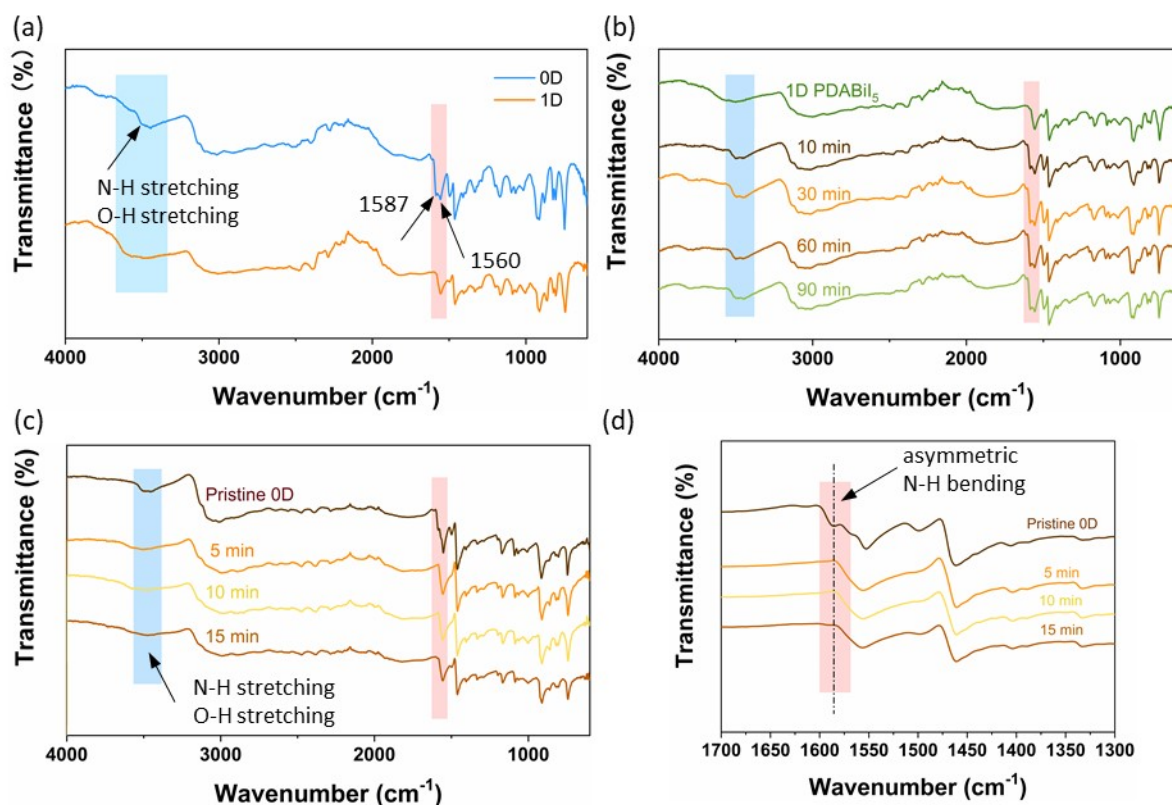


Fig. S3. (a) FTIR spectra of 1D and 0D powders. (b) FTIR spectra of 1D powder samples exposed to humid air (70% humidity) for 10 min, 20 min, 30 min, 60 min, and 90 min. (c) FTIR spectra of 0D powder being heated at 120 °C for certain periods (0 min, 5 min, 10 min and 15 min), and (d) a zoom-in range of 1300 -1700 cm^{-1} for 0D and heated samples.

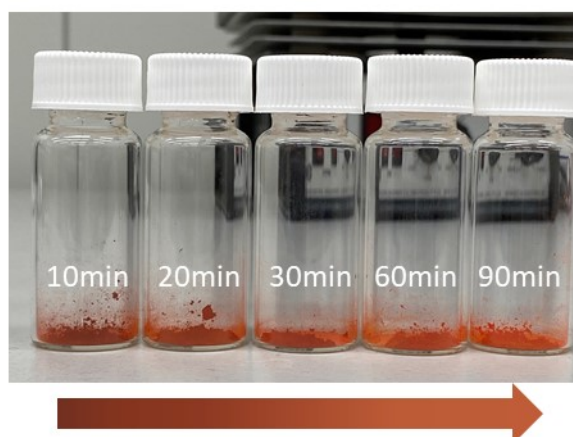


Fig. S4. Images of 1D powder samples exposed to humid air (70% humidity) for 10 min, 20 min, 30 min, 60 min, and 90 min. The sample color turned from dark to light after exposure to humidity, suggesting the gradual structure conversion from 1D to 0D.

Dual-peak PL emissions were found on 1D single crystal. The possibility of mixed compositions on the crystal surface causing dual PL emission was ruled out by conducting confocal PL mapping on a 1D single crystal, as shown in **Fig. S5**. Emissions of 563 nm and 683 nm uniformly distribute over the crystal surface which strongly confirms the origin of these emissions is from the sample without the presence of any other possible composition. Moreover, these peak positions are inconsistent with those of 0D, so there is no existence of the 0D phase in the bulk crystal. Besides, well-matched XRD patterns in **Fig. S2** also confirmed the crystal is a single component.

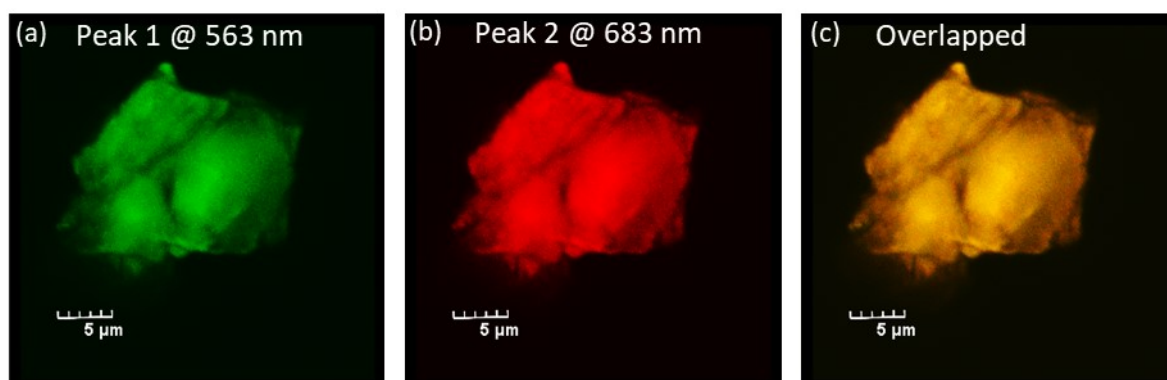


Fig. S5. Single-wavelength confocal PL mapping of a 1D single crystal at (a) 563 nm, (b) 683 nm, and (c) the sum emission considering both peaks.

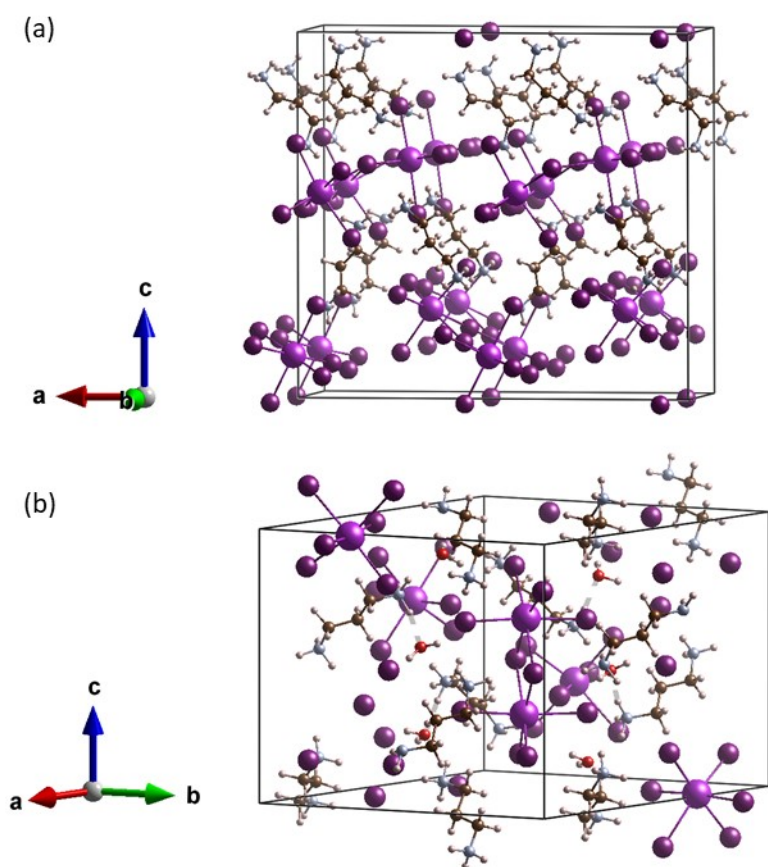


Fig. S6. Crystal structures used in DFT calculations. (a) 1D crystal structure and (b) 0D crystal structure.

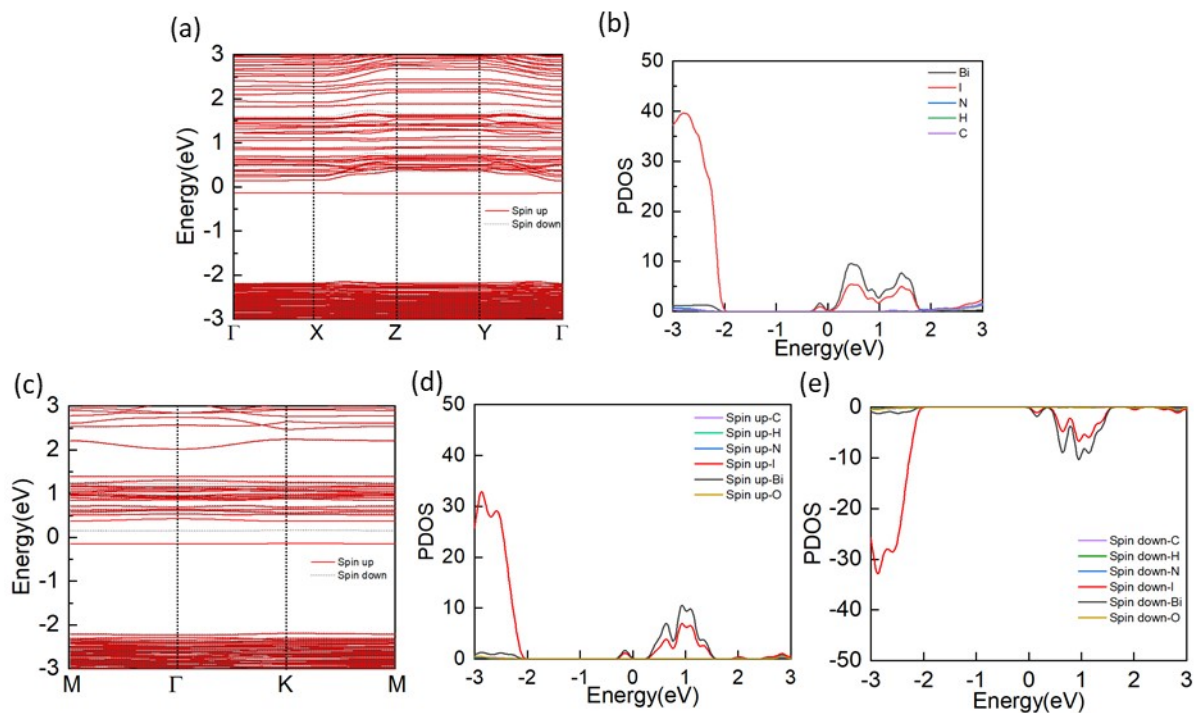


Fig. S7. (a) Spin polarized band structure and (b) element projected density of states (spin up channel) for the 1D structure with I vacancies. (c) Spin polarized band structure and element projected density of states (d) spin up channel and (e) spin down channel for the 0D structure with I vacancies.

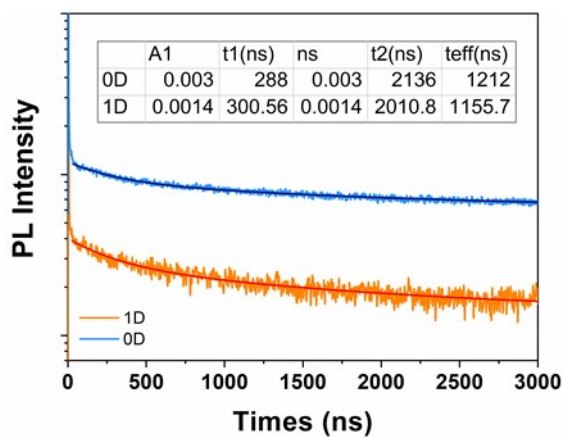


Fig. S8. Time-resolved PL decay curves of 1D and 0D materials.

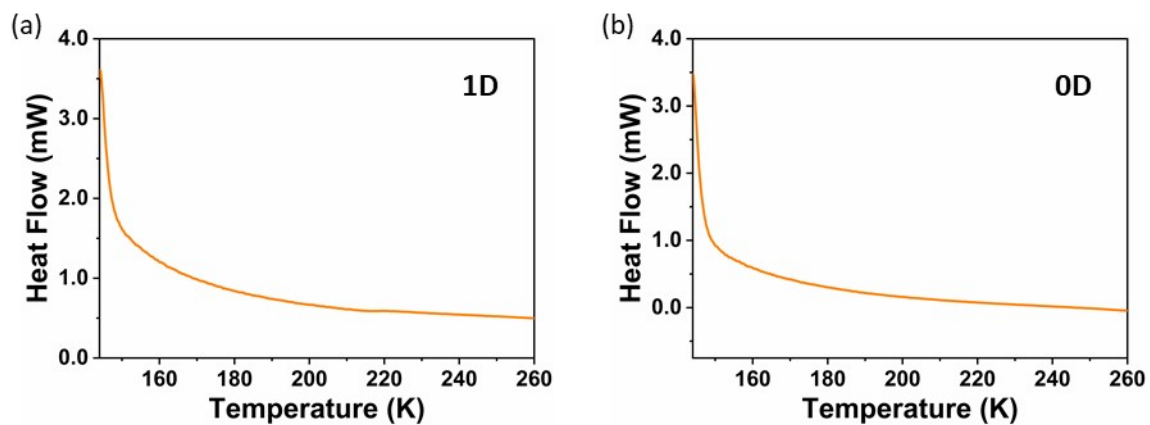


Fig. S9. Low-temperature DSC curves of (a) 1D powder and (b) 0D powder.

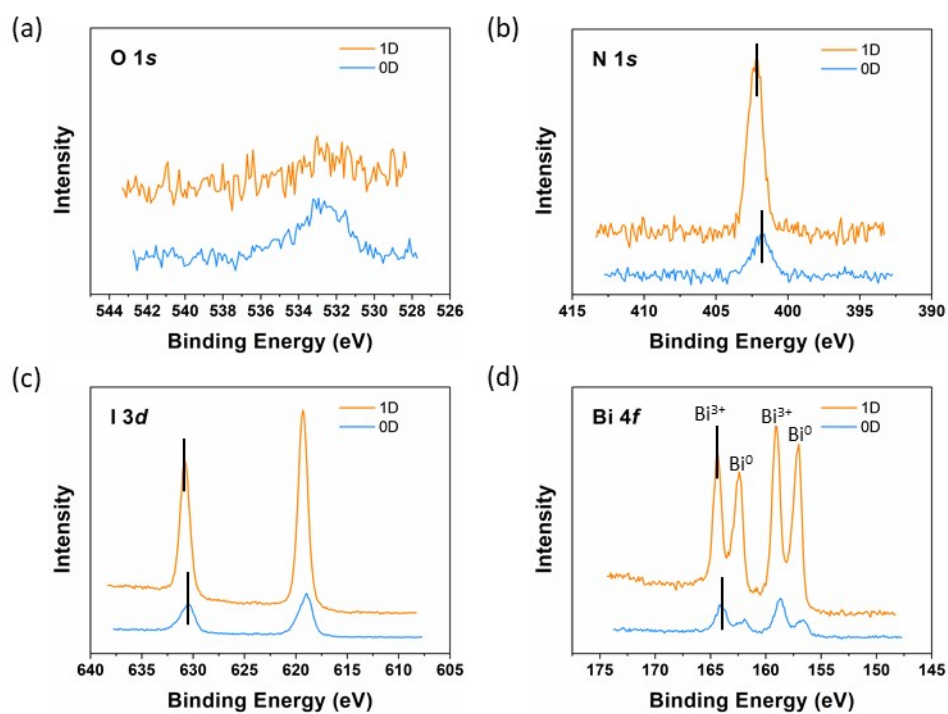


Fig. S10. XPS patterns of the 1D and 0D samples: (a) O 1s, (b) N 1s, (c) I 3d and (d) Bi 4f.

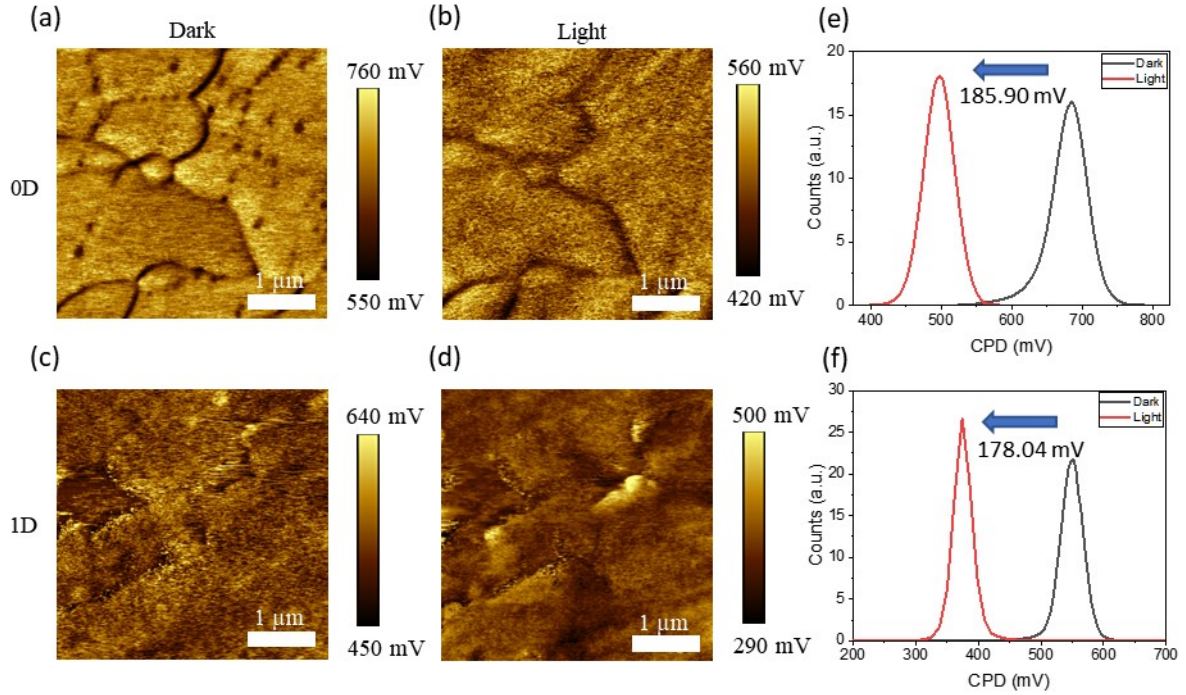


Fig. S11. KPFM images of CPD mapping measured in dark condition of (a) 0D and (c) 1D single crystals. CPD mapping images measured under while LED illumination of (b) 0D and (d) 1D single crystals. CPD statistical distribution derived from KPFM images measured under dark and illuminated conditions of (e) 0D and (f) 1D single crystals.

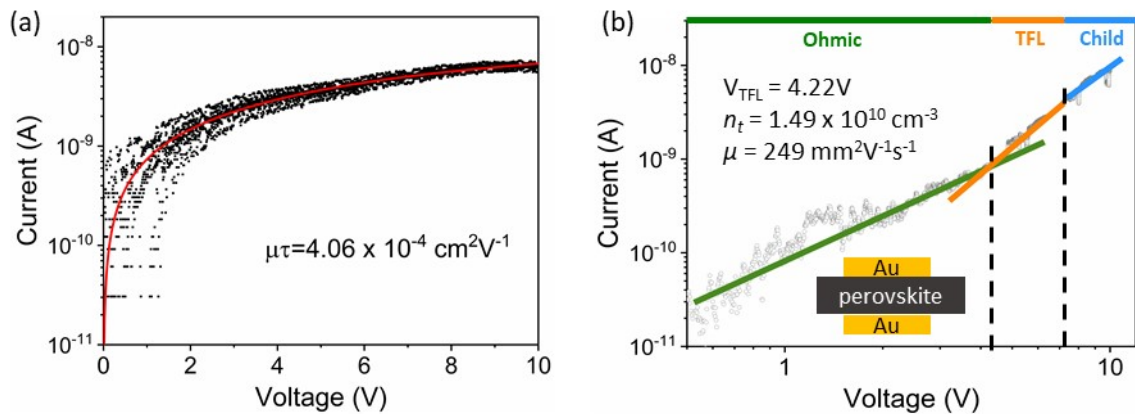


Fig. S12. (a) Light-induced IV curve and corresponding $\mu\tau$ product for Au/PDABiI₅ single crystal/Au device. (b) SCLC measurement of the PDABiI₅ single crystal-based hole-only device (the inset showing the device structure).

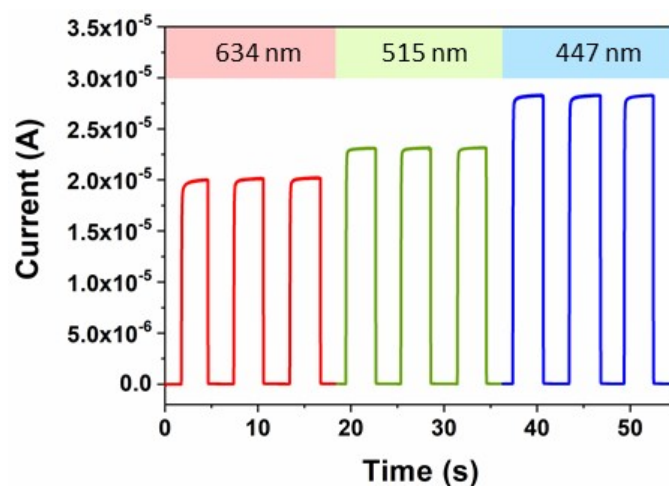


Fig. S13. ON/OFF light response of a PDABi₅ single crystal-based photodetector device. The photocurrent was measured under 634 nm, 515 nm and 447 nm wavelength illumination respectively, with the light intensity of 1 mW cm⁻² at 1V bias.

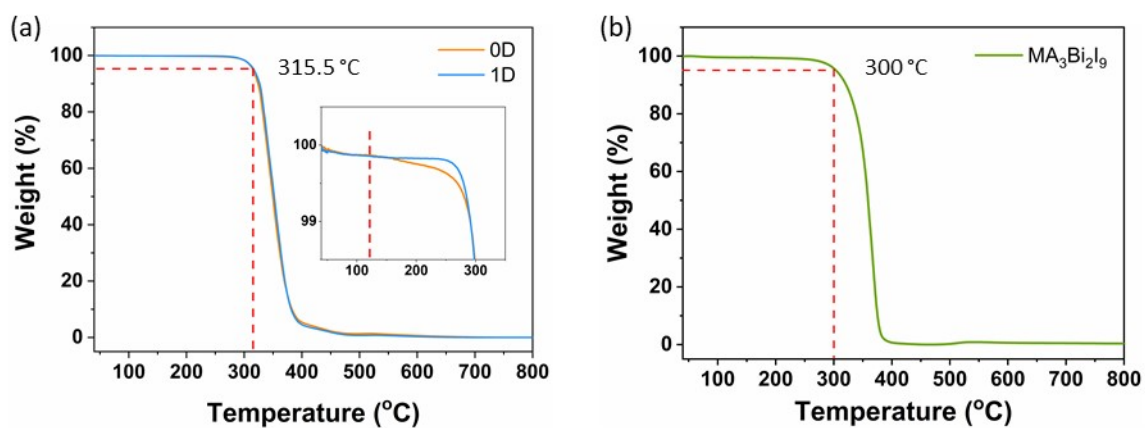


Fig. S14. (a) TGA curves of 0D and 1D powders. (b) TGA curve of MA₃Bi₂I₉ powder.

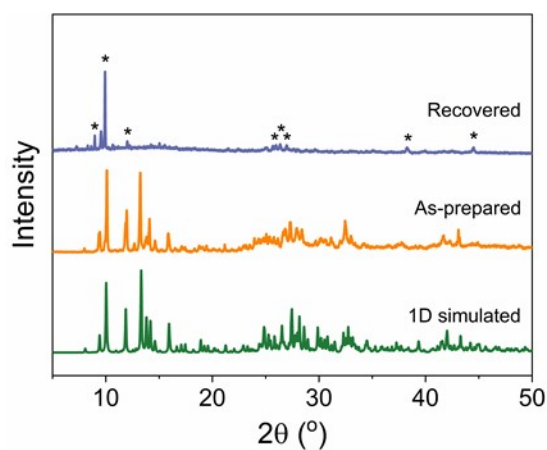


Fig. S15. XRD patterns of the as-prepared 1D powder and the recovered powder from water soaking, where stars denote characteristic peaks of 1D. To obtain the recovered powder for XDR, 1D powder was soaked in DI water for 8 days followed by filtering and drying in the oven.

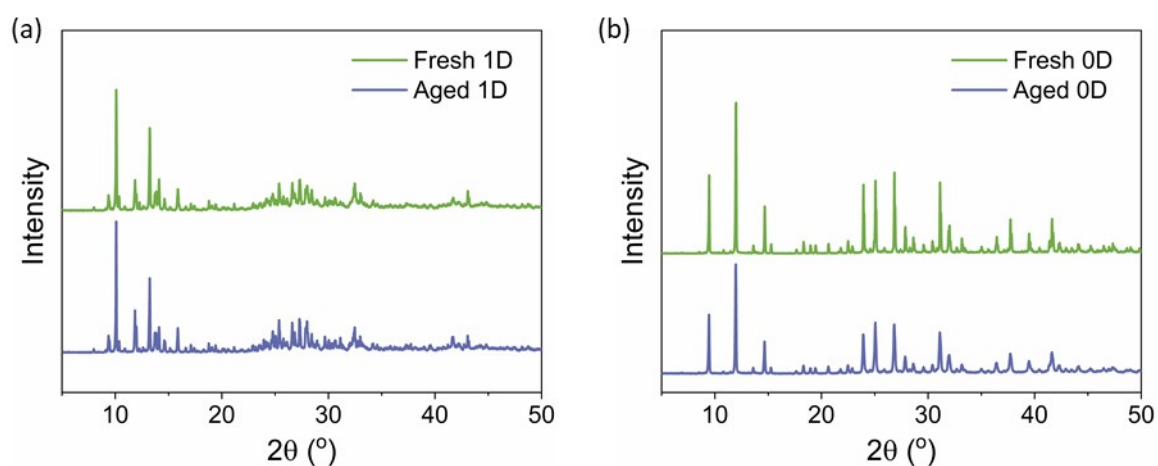


Fig. S16. XRD patterns of fresh and aged 1D and 0D samples. The aged 1D sample was stored in the glovebox for 5 months, while the aged 0D sample was stored in the ambient air for over 8 months without any change.

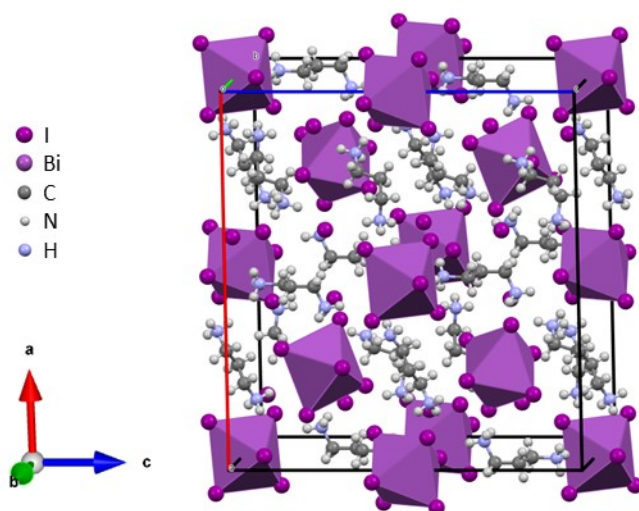


Fig. S17. The crystal structure of $\text{PDA}_5\text{Bi}_2\text{I}_{16}$.

Table S1. Crystallographic Structural Parameters of PDABiI₅, PDA₅Bi₂I₁₆ and PDA₂Bi₂I₁₀·2H₂O.

Material	PDABiI ₅ (CCDC 2348711)	PDA ₅ Bi ₂ I ₁₆ (CCDC 2348714)	PDA ₂ Bi ₂ I ₁₀ ·2H ₂ O (published) ⁵
Empirical formula	C ₃ H ₁₂ Bi I ₅ N ₂	C ₁₅ H ₆₀ Bi ₂ I ₁₆ N ₁₀	C ₆ H ₂₄ Bi ₂ I ₁₀ N ₄ O ₂
Formula weight	919.63	2829.09	1871.25
Temperature	190(2) K	190(2) K	293(2) K
Wavelength	1.54184 Å	1.54184 Å	0.71073 Å
Crystal system	Orthorhombic	Monoclinic	Trigonal
Space group	<i>Pca</i> 2 ₁	<i>I</i> 2/ <i>a</i>	<i>P</i> 3 ₁ 2 1
Unit cell dimensions	a = 22.1548(8) Å b = 8.3539(3) Å c = 70.4523(17) Å	a = 23.2806(3) Å b = 11.6357(2) Å c = 21.7251(3) Å β = 90.515(1)°	a = 14.7769(7) Å b = 14.7769(7) Å c = 13.6748(9) Å
Volume	13039.2(7) Å ³	5884.79(15) Å ³	2585.9(3) Å ³
Z	32	4	3
Density (calculated)	3.748 Mg/m ³	3.193 Mg/m ³	3.605 Mg/m ³
Absorption coefficient	95.324 mm ⁻¹	77.686 mm ⁻¹	19.157 mm ⁻¹
F(000)	12544	4936	2400
Crystal size	0.405 x 0.123 x 0.030 mm ³	0.488 x 0.322 x 0.140 mm ³	0.25 x 0.05 x 0.05 mm ³
Theta range for data collection	3.764 to 62.491°.	3.798 to 64.995°.	3.134 to 24.998°.
Index ranges	-25<=h<=0, -9<=k<=9, 0<=l<=81	-27<=h<=27, -13<=k<=13, -21<=l<=25	-17<=h<=17, -17<=k<=17, -16<=l<=16
Reflections collected	15143	13692	44044
Independent reflections	10405 [R(int) = 0.0707]	4993 [R(int) = 0.0899]	3042 [R(int) = 0.0858]
Completeness to theta = 62.491°	99.00%	99.70%	99.8%
Absorption correction	Analytical	Analytical	Semi-empirical from equivalents
Max. and min. transmission	0.165 and 0.002	0.05 and 0.002	0.995 and 0.955
Refinement method	Full-matrix least-squares on F ²	Full-matrix least-squares on F ²	Full-matrix least-squares on F ²
Data / restraints / parameters	10405 / 197 / 593	4993 / 0 / 198	3042 / 1 / 110
Goodness-of-fit on F ²	1.041	1.087	1.043
Final R indices [I>2σ(I)]	R1 = 0.1031, wR2 = 0.2625	R1 = 0.0861, wR2 = 0.2178	R1 = 0.0319, wR2 = 0.0650
R indices (all data)	R1 = 0.1163, wR2 = 0.2726	R1 = 0.0881, wR2 = 0.2222	R1 = 0.0444, wR2 = 0.0704
Largest diff. peak and hole	5.395 and -3.364 e.Å ⁻³	4.788 and -4.799 e.Å ⁻³	1.515 and -0.916 e.Å ⁻³

Table S2. Device performance of a PDABiI₅ single crystal-based photodetector. The photocurrent was measured under 634 nm, 515 nm and 447 nm wavelength illumination respectively, with the light intensity of 1 mW cm⁻² at 1V bias.

	B (447 nm)	G (515 nm)	R (634 nm)
ON/OFF ratio	812.47	665.08	582.18
EQE (%)	108.74	77.24	54.91
R (A/W)	0.39	0.32	0.28
D* (Jones)	9.96×10 ¹¹	8.15×10 ¹¹	7.14×10 ¹¹

References

1. G. Kresse and J. Furthmüller, Efficiency of ab-initio total energy calculations for metals and semiconductors using a plane-wave basis set, *Comput. Mater. Sci.*, 1996, **6**, 15-50.
2. G. Kresse and J. Furthmüller, Efficient iterative schemes for ab initio total-energy calculations using a plane-wave basis set, *Phys. Rev. B*, 1996, **54**, 11169.
3. P. E. Blöchl, Projector augmented-wave method, *Phys. Rev. B*, 1994, **50**, 17953.
4. J. P. Perdew, K. Burke and M. Ernzerhof, Generalized gradient approximation made simple, *Phys. Rev. Lett.*, 1996, **77**, 3865.
5. J. K. Pious, A. Katre, C. Muthu, S. Chakraborty, S. Krishna and C. Vijayakumar, Zero-dimensional lead-free hybrid perovskite-like material with a quantum-well structure, *Chemistry of Materials*, 2019, **31**, 1941-1945.